Radioactive iodine migration in zirconia and its affect on waste storage materials

F. Brossard[1], A. Chevarier[1], N. Chevarier[1], N. Moncoffre[1], D. Crusset[2], H. Faust[3], Ph. Sainsot[4]

[1] *Institut de Physique Nucléaire de Lyon, IN2P3/CNRS, Université Claude Bernard, F-69622 Villeurbanne Cedex, France*

[2] *ANDRA, Parc de la croix Blanche, F-92298 Châtenay-Malabry Cedex, France*

[3] *Institut Laue-Langevin, B.P. 156, F-38042 Grenoble Cedex 9, France*

[4] *Institut National des Sciences Appliquées F-69621 Villeurbanne Cedex, France*

Abstract

During the reactor operation, fission products are implanted by recoil inside the zircaloy cladding tube. Most of them are distributed in the first 2 μm. At the same time oxidation of the cladding tube occurs, hence in the waste storage phase zirconia will act as a migration barrier. In order to analyse the mechanism involved in iodine migration, stable and radioactive iodine atoms are implanted in zirconium oxidized samples. Iodine thermal-release is measured either by Rutherford Backscattering Spectrometry or γ spectroscopy. Two depth ranges are studied, the near surface (<400 nm) and the one micrometer mean range. The analysis of the iodine migration data so obtained allows to determine the role of diffusion processes in iodine release.

INTRODUCTION

The large uranium fission cross section leads to long lived fission products like iodine, and the behaviour of these elements in the cladding tube during energy production and afterwards during waste storage is a crucial problem (1, 2). During the reactor processing, fission products are implanted by recoil inside the zircaloy cladding tube at different energies ranging from keV to some tens of MeV. This corresponds to implanted depths varying, respectively, from 10 nm to several μm (3-5).

Let us first remind that in France nuclear wastes are classified into 3 categories depending on the type and on the importance of radioactivity (α, β, γ radiation and high, medium, low activities). They are then specifically deposited. High level nuclear wastes belong to the C category made of fission products, actinides and activation products. Among fission products, iodine poses a real problem first, because it is a volatile element and secondly because ^{129}I has a very long half life ($T=1.59 \times 10^7$ years). At the moment, two storage options are opened : the closed cycle for which wastes are reprocessed and the open cycle, where no reprocessing is performed. In the open cycle, the spent fuel UO_2 forms directly the first barrier to radionuclide migration surrounded by a second barrier which is the zircaloy cladding tube. In the closed cycle, fission products and minor actinides are separated from uranium and plutonium and then vitrified to constitute the waste glasses. Before chemical separation the cladding tubes are sectioned into pieces called hulls in order to release the UO_2 pellets which are rendered

soluble in nitric acid. The hulls are collected as solid wastes and embedded inside a concrete structure. In the perspective of geological storage, a great interest is given to migration processes in order to model and to extrapolate them to large time scales (6).

We have focused this study on iodine migration into zirconia (zirconium oxide) since a natural oxidation of the internal face of the zircaloy tube occurs during reactor operation simply by contact with the UO_2 fuel on a thickness ranging between 5 and 10 μm (7). Hence fission products are implanted in the superficial ZrO_2 layer. The mean energy of emitted fission products from UO_2 is 73 MeV, and their maximum range inside the cladding tube is about 7 μm. However, most of them are distributed in the first 2 μm. For these reasons it is of primary importance to study phenomena occurring at the surface of the cladding tube. The aim of this work is to study iodine diffusion into zirconia by using ion implantation. This method allows to introduce impurity atoms in a solid with an excellent control of depth and concentration by adjusting incident energy and fluence (8,9). Two types of implantation have being carried out using either stable or radioactive isotopes. For each implantation condition successive annealings were carried out. In case of stable isotopes Rutherford Backscattering Spectrometry (RBS) was used in order to determine the iodine implantation profiles corresponding to each annealing parameter (temperature, time). It allowed to analyse the migration process through both the evolution of iodine profiles and the mean iodine release, and to get the signature of the involved process. The only drawback of coupling stable iodine implantation and RBS is the high implantation dose required because of the lack of sensitivity in RBS profiling (around 10^{16} at.cm^{-2} which is much larger than the cladding tube content of about 10^{14} at.cm^{-2}).Therefore radioactive ion implantation involving doses less than 10^{9} at.cm^{-2} was performed. In this case, the radioactivity release was measured by γ spectroscopy, and analysed in terms of a diffusion process. It is well known that irradiations as well as hydriding effects enhance significantly the corrosion rate of cladding tubes (10,11). In this study their influence upon diffusion phenomena has not been taken into account.

MIGRATION STUDY USING STABLE IODINE IMPLANTATION

In this section, the mechanisms involved in iodine migration are studied analyzing both the evolution of concentration profiles and the iodine release rate as a function of annealing conditions. The 800 keV stable ^{127}I implantations were performed on the isotope separator of the 'Institut de Physique Nucléaire' of Lyon (IPNL). Iodine implantation parameters calculated from the TRIM code (12) are the mean range R_p and the straggling σ of the iodine distribution which are 164 nm and 52 nm, respectively.

The time evolution of iodine experimental profiles measured by RBS in case of 750°C and 800°C annealings are displayed by dots in figure 1 (a, b). A strong iodine release occurs after 5 minutes annealing. No distortion of the gaussian shape distribution is observed, which means that the iodine release concerns the whole implantation depth. After this rapid process, a much slower one takes place which can be related to diffusion. The evolution of the iodine profile as well as of the iodine release is interpreted in terms of a diffusion mechanism, using a numerical resolution of Fick's law which is now described.

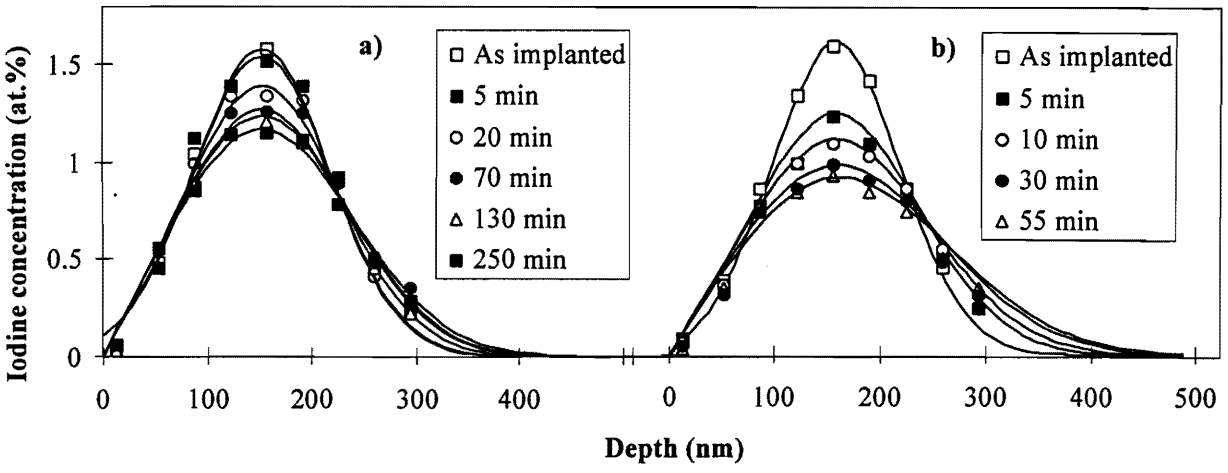

Figure 1 : Evolution of the 800 keV iodine concentration profiles at 750 and 800°C as function of the annealing time. Dots represent RBS experimental profiles and full curves are the calculation results.

Analysis of the distribution profiles

Fick's second law is given by : $\frac{\partial C}{\partial t} = D\frac{\partial^2 C}{\partial x^2}$ (1)

where C is the concentration of the diffusing species and D is the diffusion coefficient. Solutions depend on boundary conditions.

Let us assume that the initial condition is given by the implanted iodine distribution defined by its gaussian shape:

$$C(x,0) = C_m \exp -\frac{(x - Rp)^2}{2\sigma^2} \qquad (2)$$

where R_p is the projected implantation range and σ the straggling. C_m is the iodine concentration at $x = R_p$. The boundary conditions corresponding to the experiments are : $C(\infty,t)=0$ and $C(0,t) = 0$.

Let us consider Fick's second law with non dimensioned variables.

$\bar{x} = \frac{x}{\sigma}$, $\bar{C} = \frac{C}{C_m}$, where σ is the straggling, and C_m the iodine concentration at $x = R_p$

Therefore : $\frac{\partial^2 \bar{C}}{\partial \bar{x}^2} = \frac{\sigma^2}{D}\frac{\partial \bar{C}}{\partial t}$

setting $\bar{t} = \frac{tD}{\sigma^2}$, then $\frac{\partial^2 \bar{C}}{\partial \bar{x}} = \frac{\partial \bar{C}}{\partial \bar{t}}$

The integration is performed using the finite difference method with the explicit scheme :

$$\frac{\partial^2 \bar{C}}{\partial \bar{x}^2} = \frac{\bar{C}_{i+1}^{t=n} - 2\bar{C}_i^{t=n} + \bar{C}_{i-1}^{t=n}}{\Delta \bar{x}^2} \quad \text{and} \quad \frac{\partial \bar{C}}{\partial \bar{t}} = \frac{\bar{C}_i^{n+1} - \bar{C}_i^n}{\Delta \bar{t}}$$

where i and n correspond, respectively, to the iterative procedure on depth and time with a step r, $r = \frac{\Delta\bar{t}}{\Delta\bar{x}^2}$ with $r < 1/2$

Therefore $\bar{C}_i^{n+1} = (1-2r)\bar{C}_i^n + r(\bar{C}_{i-1}^n + \bar{C}_{i+1}^n)$

Starting from the initial implanted distribution, the time $\bar{t}$ necessary to fit correctly the distribution profile after an annealing time t, allows to deduce the diffusion coefficient, D since $D = \frac{\bar{t}\sigma^2}{t}$

The fits obtained using such a numerical approach are given in figure 1 (a, b) by full lines. It shows clearly that the predicted broadening due to diffusion process is slightly larger than the experimental one, and experimental data are quite well reproduced by the simulation. In addition, figure 2 which represents D as function of annealing time at 750 and 800°C, puts in evidence that two processes are involved : i) a rapid one occurring in the first five minutes and ii) a slower one which can be attributed to a diffusion process. A behavior like in i) has been observed in hydrogen and deuterium release (13, 14) and was interpreted as a release of non bound atoms.

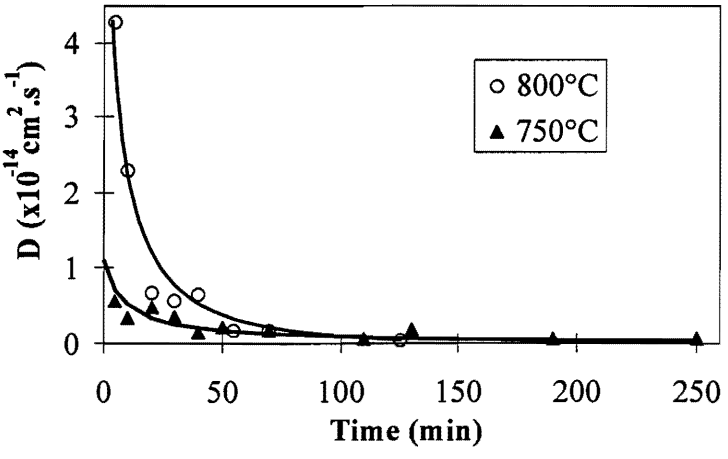

Figure 2 : Diffusion coefficients versus time for the 750 and 800°C annealings.

For each temperature, two mean diffusion coefficients are deduced for the rapid and for the slow diffusion processes. At 750°C, they are respectively of $5x10^{-15}$ and $5x10^{-16}$ cm^2 s^{-1} and at 800°C, they are of 10^{-14} and 10^{-15} cm^2 s^{-1}. The ratio between the rapid and the slow phase corresponds to about one order of magnitude.

Analysis of the iodine release

The desorption rate is determined experimentally using integration of the trapped iodine concentration over the depth profile. Let us note N(0) the iodine concentration measured by RBS in the implanted sample, and N(t) the iodine concentration measured after an annealing time t.

Hence : $Y(t) = \frac{N(0) - N(t)}{N(0)}$

The experimental desorption rates are represented by dots in figure 3 as function of the annealing times for temperatures at 750 and 800°C.

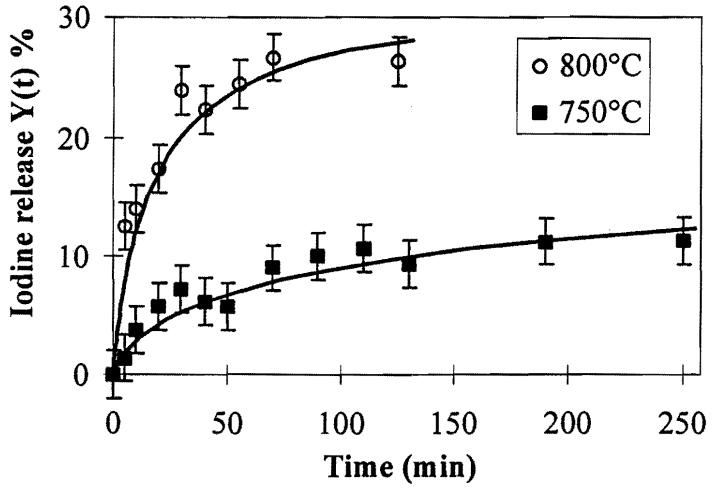

Figure 3 : Iodine release versus the annealing time at 750 and 800°C

In a second step, from the initial iodine distributions given by the TRIM code which fit well with the experimental RBS profiles, we have used the diffusion coefficients D deduced previously to calculate the iodine release predicted by Fick's second law. The results are represented by the continuous lines in figure 3. The good agreement obtained allows to validate this calculation procedure.
This shows that this numerical resolution of the diffusion equation can be used in order to reproduce the iodine release, starting from the TRIM predicted profiles.

MIGRATION STUDY USING RADIOACTIVE IODINE IMPLANTATION

The 6.5 MeV implantations were realised by using the Lohengrin spectrometer at ILL from the neutron induced fission of ^{239}Pu. The Lohengrin spectrometer allows to select the 133 isobaric chain at an energy of 65 MeV and an ionic charge of 24, which corresponds to the highest intensity. The use of a 8 μm thick aluminium absorber allows to decrease the incident energy to 6.5 MeV. The layer thickness was checked by using α emission from ^{241}Am at 5.486 MeV. After an irradiation time of 11h 30min, the fluence was found to be approximately $1.6x10^{7}$ at.cm^{-2} which corresponds to a maximum iodine concentration of $2x10^{-10}$ at. %.

The 133 isobaric chain has the following decay characteristics (15) :

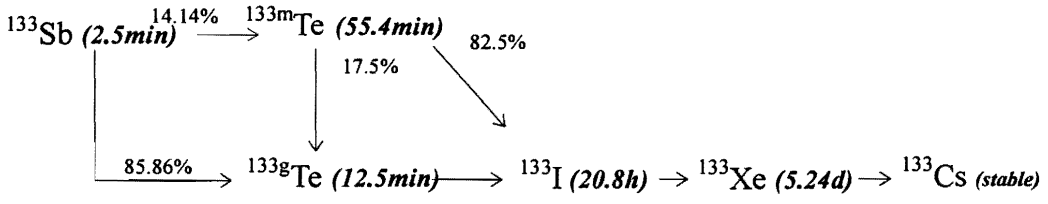

Activities of the different radionuclides were followed by γ spectroscopy using a Ge(HP) detector with 2 keV resolution:

^{133m}Te : Eγ = 913 keV and 334 keV ; - ^{133g}Te : Eγ = 312 keV,
^{133}I : Eγ = 530 keV ; - ^{133}Xe : Eγ = 81 keV.

The evolution of the ^{133}I activity has been determined by integrating the filiation equations. Measurements of γ rays have been normalised from these calculated activities taking as a reference the activities of non annealed samples. These results have been published (16) and it was shown that the iodine release is deduced from comparison between the experimental data and the calculated activities. This iodine release is plotted in Figure 4 in case of the 800°C annealing and compared to the 800 keV results. For annealing temperatures lower than 800°C, no desorption is observed in the studied time scale whatever the sample nature.

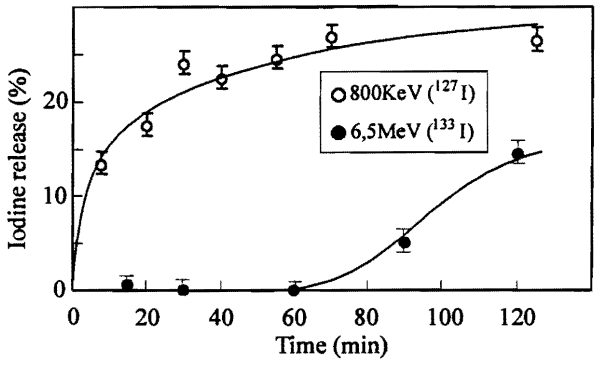

Figure 4 : Iodine release versus annealing time for 800 keV and 6.5 MeV implantations.

By using the previously described numerical procedure it is possible to reproduce the 90 minute delay time necessary to observe iodine desorption in case of 6.5 MeV implantation. These results can be understood by focusing on the rapid desorption phase. Let us consider Fick's second law (equation (1)) with non dimensioned variables. For a given experiment :

$$\bar{x} = \frac{x}{\sigma}, \qquad \bar{C} = \frac{C}{C_m}, \qquad \text{and} \qquad \bar{t} = \frac{t}{\tau}$$

where σ is the straggling, τ the time necessary to observe iodine desorption and C_m the iodine concentration at $x=R_p$.

Therefore : $$\frac{\partial^2 \bar{C}}{\partial \bar{x}^2} = \frac{\sigma^2}{D\tau} \frac{\partial \bar{C}}{\partial \bar{t}}$$

For two different experiments numbered 1 and 2 : $$\frac{\sigma_1^2}{D_1\tau_1} = \frac{\sigma_2^2}{D_2\tau_2} = \text{constant}$$

If we compare the experiments performed at ILL (labelled 1) with the ones at 800 keV (labelled 2), for an annealing temperature of 800°C, we can write :

$D_1 = D_2$, hence : $$\frac{\sigma_1^2}{\tau_1} = \frac{\sigma_2^2}{\tau_2}$$

Since σ_1 = 500 nm, σ_2 = 52 nm and from the fact that about 90 minutes were necessary at ILL to observe a desorption (τ_1 = 90 min), we can deduce that only one minute is necessary at

800 keV to observe iodine release (τ_2 = 1 min). The sensitivity of the technique does not allow to determine such a short time and this explains why the iodine release appears to be immediate.

CONCLUSIONS

The interpretation of both evolution of iodine profiles and iodine releases has been performed by using a numerical integration of Fick's second law. A two step process has been put in evidence. The diffusion coefficient ratio between the rapid and the slow phase thus deduced corresponds to about one order of magnitude. The rapid iodine release has been attributed to a desorption of non bound iodine atoms. Complementary experiments are being performed with the purpose to correlate iodine desorption with the defect density created either by atomic bombardment or by electron irradiation. The first results obtained by grazing angle X-ray diffraction seem to show that this release is related to a recrystallisation of the surface oxide layer as well as to a grain growth.
For assessing the long term safety of hulls and cups storage in a geological repository, possible release of iodine 129 and its transport from the disposal to some outlets of the geosphere over periods of time as long as 10^6years are considered. The very small D values obtained in the slow phase assess of low risk. However defects induced by irradiation either during energy production or during the storage phase could enhanced the iodine diffusion. Experiments including either atomic or electron irradiation are in progress.

REFERENCES

1. V.M Oversby, Mat. Science Tech., 10B, 392-439 (1994).
2. R. C Ewing, , W.J Weber, and F.W Clinard, Prog. Nucl. Energy, 29 (2), 63-127 (1995).
3. T Hirabayashi, T Sato, C. N Sagawa, M Masaki, M. Saeki, and T. Adachi, J. Nucl. Mater., 174, 45-52 (1990).
4. M.Fregonese, « Mécanisme de corrosion sous contrainte par l'iode dans le zirconium et le zircaloy-4. Transposition aux conditions d'interaction pastille-gaine dans les réacteurs à eau pressurisée », Thesis, Institut National Polytechnique of Grenoble, France. October 1997.
5. R.Restani, E. T. Aerne, G.Bart, H. P. Linder, A. Müller, F.Petrik, Technical Report 92-13, Nagra, Wettingen, Switzerland, 1992.
6. H. Kleykamp, J. Nucl. Mater., 171, 181-188 (1990).
7. H. Matzke, J. Nucl. Instr. and Meth. in Phys. Res., B32, 455-470 (1988).
8. N. Moncoffre, A. Chevarier, N. Chevarier, N. Millard-Pinard, International Workshop on Research with fission fragments, ED. T. Von Egidy, D. Habs, F. J. Hartmann, K. E. G. Löbner, H. Niefnecker, World Scientific, 1997, pp. 287-292.
9. N. Chevarier, F. Brossard, A. Chevarier, D. Crusset, N. Moncoffre, Nucl. Instr. and Meth.in Phys. Res.B136-138, 784-787 (1998).
10. F.Lefebvre, C. Lemaignan, J.nucl. Mater., 248,268-274 (1997).
11. M. Blat, J. Bourgoin EDF report n° HT-45/97/007/A,1997
12. J. P Biersack, L. G. Haggmark,., Nucl. Instr. and Meth. 174, 257 (1980)..
13. F. Schiettekatte, D. Keroack, G. Ross, B.Terreault, Nucl. Instr. and Meth B90,401 (1994).

14. E. Murch, Mat. Science Tech., **5**, 77-124 (1994).
15. J.A Turnbull, C.A Friskney, J.R. Findlay, F.A . Johnson, and A.J. Walter, J. Nucl. Mater., 107, 168-184 (1982).
16. F. Brossard, G. Carlot, A. Chevarier, N. Chevarier, D. Crusset, J.C. Duclot, H. Faust, C. Gaillard, N. Moncoffre, Proceedings of the 2nd International Workshop on Nuclear Fission and Fission-Product Spectroscopy, April 1998.